EXHIBIT 5

scattering realization. Also plotted in Fig. 3 for comparison are results from effective medium theories (*22*, *23*), which depend only on the porosity and refractive index ratio. The morphology of the scattering material determines which effective medium model is applicable (*22*). Maxwell Garnett theory was developed for spherical scatterers in a homogeneous dielectric background (*22*), whereas Bruggeman's approach (*16*) treats both dielectric components on a symmetrical basis and seems to be the better choice for porous GaP. Both the porosity and the refractive index ratios of our samples are known. The two effective medium theories are compared with experimental results without any adjustable parameters. As can be seen, our measurements are not quantitatively described by existing effective medium models, which prompts the need to develop new theories. In fact, an effective medium approach is not expected to apply, because it was developed for weakly scattering media with $s \ll \lambda$ and relatively small m. It is therefore not surprising that the discrepancy between theory and experiment is largest for the most strongly scattering material, PA-GaP. As observed, a relatively small decrease in refractive index ratio, from 3.26 to 2.12, leads to a large modification of the scattering efficiency, establishing the importance of the refractive index ratio for strongly photonic materials.

References and Notes

1. E. Yablonovitch, *Phys. Rev. Lett.* **58**, 2059 (1987); S. John, *ibid.*, p. 2486.
2. B. T. Holland, C. F. Blanford, A. Stein, *Science* **281**, 538 (1998); J. E. G. J Wijnhoven and W. L. Vos, *ibid.*, p. 802.
3. P. W. Anderson, *Phys. Rev.* **109**, 1492 (1958); S. John, *Phys. Rev. Lett.* **53**, 2169 (1984); P. W. Anderson, *Philos. Mag. B* **52**, 505 (1985).
4. D. S. Wiersma, P. Bartolini, A. Lagendijk, R. Righini, *Nature* **390**, 671 (1997).
5. U. Grüning, V. Lehmann, S. Ottow, K. Busch, *Appl. Phys. Lett.* **68**, 747 (1996).
6. D. E. Aspnes and A. A. Studna, *Phys. Rev. B* **27**, 985 (1983).
7. B. D. Chase and D. B. Holt, *J. Electrochem. Soc.* **119**, 314 (1972).
8. B. H. Erné, D. Vanmaekelbergh, J. J. Kelly, *Adv. Mater.* **7**, 739 (1995).
9. F. Iranzo Marín, M. A. Hamstra, D. Vanmaekelbergh, *J. Electrochem. Soc.* **143**, 1137 (1996).
10. C. Zener, *Proc. R. Soc. London* **145**, 523 (1934).
11. D. Vanmaekelbergh and L. van Pieterson, *Phys. Rev. Lett.* **80**, 821 (1998).
12. W. Bresser, P. Boolchand, P. Suranyi, *ibid.* **56**, 2493 (1986).
13. B. E. Warren, *X-ray Diffraction* (Dover, New York, 1990).
14. From previous electrochemical experiments, it is known that the photoanodic etching current density at this wavelength was below the detection limit, indicating that the amount of light absorption is undetectably small.
15. A. Ishimaru, *Wave Propagation and Scattering in Random Media*, vols. I and II (Academic Press, New York, 1978); A. Z. Genack, *Phys. Rev. Lett.* **58**, 2043 (1987).
16. P. Sheng, *Introduction to Wave Scattering, Localization, and Mesoscopic Phenomena* (Academic Press, San Diego, CA, 1995).
17. A. Lagendijk, R. Vreeker, P. de Vries, *Phys. Lett. A* **136**, 81 (1989).
18. J. X. Zhu, D. J. Pine, D. A. Weitz, *Phys. Rev. A* **44**, 3948 (1991).
19. D. J. Durian, *Phys. Rev. E* **50**, 857 (1994).
20. For A-GaP, n_e, which depends on the porosity, is estimated to be 2.0 ± 0.1, corresponding to z_e = 5.4 ± 0.6. Whereas for the higher porosity medium, PA-GaP, n_e = 1.7 ± 0.1 and thus z_e = 3.4 ± 0.5.
21. D. S. Wiersma, M. P. van Albada, B. A. van Tiggelen, A. Lagendijk, *Phys. Rev. Lett.* **74**, 4193 (1995).
22. R. Landauer, *Electrical Transport and Optical Properties of Inhomogeneous Media*, J. C. Garland and D. B. Tanner, Eds. [American Institute of Physics (AIP) Conference Proceedings No. 40, AIP, New York, 1978)].
23. W. Lamb, D. M Wood, N. W. Ashcroft, *Phys. Rev. B* **21**, 2248 (1980); S. Datta, C. T. Chan, K. M. Ho, C. M. Soukoulis, *ibid.* **48**, 14936 (1993); K. Busch and C. M. Soukoulis, *Phys. Rev. Lett.* **75**, 3442 (1995).

24. We thank J. Gómez Rivas for valuable discussions, P. de Jongh for taking the SEM pictures, and Philips Research Laboratories (Eindhoven, The Netherlands) for supplying the GaP crystals. This work is part of the research program of the Stichting voor Fundamenteel Onderzoek der Materie, which is financially supported by the Nederlandse Organisatie voor Wetenschappelijk Onderzoek.

24 December 1998; accepted 1 March 1999

Multilineage Potential of Adult Human Mesenchymal Stem Cells

Mark F. Pittenger,[1]* Alastair M. Mackay,[1] Stephen C. Beck,[1] Rama K. Jaiswal,[1] Robin Douglas,[1] Joseph D. Mosca,[1] Mark A. Moorman,[1] Donald W. Simonetti,[1] Stewart Craig,[1] Daniel R. Marshak[1,2]

Human mesenchymal stem cells are thought to be multipotent cells, which are present in adult marrow, that can replicate as undifferentiated cells and that have the potential to differentiate to lineages of mesenchymal tissues, including bone, cartilage, fat, tendon, muscle, and marrow stroma. Cells that have the characteristics of human mesenchymal stem cells were isolated from marrow aspirates of volunteer donors. These cells displayed a stable phenotype and remained as a monolayer in vitro. These adult stem cells could be induced to differentiate exclusively into the adipocytic, chondrocytic, or osteocytic lineages. Individual stem cells were identified that, when expanded to colonies, retained their multilineage potential.

Recently, pluripotent stem cells have been cultured from human fetal tissue and have shown the ability to give rise to a variety of differentiated cell types found in embryonic germ layers (*1*). Many adult tissues contain populations of stem cells that have the capacity for renewal after trauma, disease, or aging. The cells may be found within the tissue or in other tissues that serve as stem cell reservoirs. For example, although bone marrow is the major source of adult hematopoietic stem cells (HSCs) that renew circulating blood elements, these cells can be found in other tissues (*2*). The adult bone marrow also contains mesenchymal stem cells (MSCs), which contribute to the regeneration of mesenchymal tissues such as bone, cartilage, muscle, ligament, tendon, adipose, and stroma (*3–5*). In vitro and animal implant studies (*5–10*) have indicated that there is either a multipotent MSC or the populations are mixtures of committed progenitor cells, each with restricted potential. We report the isolation, expansion, and characterization of the multipotent human MSC (hMSC).

We characterized an isolated population of homogeneous human mesenchymal cells from bone marrow taken from the iliac crest (*5*) (see Web Fig. 1, available at www.sciencemag.org/feature/data/983855.shl). Previous studies have identified selection criteria for fetal bovine serum (FBS) that allows the expansion of a marrow cell population with MSC potential after implantation (*5, 11*). The mesenchymal cells described here were characterized by their ability to proliferate in culture with an attached well-spread morphology (Fig. 1, A and B), by the presence of a consistent set of marker proteins on their surface (Fig. 1, C and D) (*12–14*), and by their extensive consistent differentiation to multiple mesenchymal lineages under controlled in vitro conditions (Fig. 2).

A density gradient was used in the isolation procedure to eliminate unwanted cell types that were present in the marrow aspirate. A small percentage (estimated at about 0.001 to 0.01%) of cells isolated from the density interface of 1.073 g/ml attached and grew as fibroblastic cells that developed into

[1]Osiris Therapeutics, 2001 Aliceanna Street, Baltimore, MD 21231–3043, USA. [2]Johns Hopkins University, School of Medicine, Baltimore, MD 21205, USA.

*To whom correspondence should be addressed. E-mail: mpittenger@osiristx.com

visible symmetric colonies at about 5 to 7 days after initial plating. HSCs and nonadherent cells were removed with changes in medium. The isolated cultured mesenchymal cells comprised a single phenotypic population (95 and 98% homogeneous at passages 1 and 2, respectively) by flow cytometric analysis of expressed surface antigens; whether or not trypsin was used to remove the cells from the substrate did not change the results. These expanded attached mesenchymal cells were uniformly positive for SH2, SH3, CD29, CD44, CD71, CD90, CD106, CD120a, CD124, and many other surface proteins. Immunofluorescence microscopy evaluation showed no unlabeled cells. No subpopulations of marrow-derived mesenchymal cells could be discerned morphologically by microscopic observation or by fluorescence cytometry, size, and granularity criteria, or with more than 50 available antibodies (*11, 13, 14*) (see Web Fig. 1). Several of these antibodies were used to routinely characterize the expanded mesenchymal cell population. In contrast, the mesenchymal cells were negative for other markers of the hematopoietic lineage, including the lipopolysaccharide receptor CD14, CD34, and the leukocyte common antigen CD45 (Fig. 1D). Hematopoietic cells were never identified in the expanded cultures. The mesenchymal cells appear to be different from marrow fibroblastic cells isolated by other cells that remained positive for the CD34 surface antigen (*15*). As many as 50 million to 375 million cells were generated by passage 2 from a 10-ml marrow aspirate that was obtained from 19- to 57-year-old donors (see Web Fig. 1). This range of yield is expected for the expansion of primary cells. We isolated these cells from the marrow of over 350 donors, and the expanded mesenchymal cells from at least 50 donors were tested in three lineage assays, with all tested donors responding positively in these assays. The cells did not differentiate spontaneously during culture expansion. Similarly isolated marrow mesenchymal cells maintained a normal karyotype and telomerase activity, even at passage 12 (see Web Fig. 1).

The differentiation potential of the mesenchymal cells from three adult donors were compared to two strains of human fibroblasts (*16*), which are other cells of mesenchymal lineage, by culturing the cells under conditions that were favorable for adipogenic, chondrogenic, or osteogenic differentiation. After 1 to 3 weeks in lineage-specific culture conditions, the expanded cells from the three donors were highly differentiated (the phenotype of lineage-specific cell types was easily distinguished), without evidence of the other lineages (Fig. 2, A through I).

Adipogenic differentiation was induced in the expanded mesenchymal cell cultures by treatment with 1-methyl-3-isobutylxanthine, dexamethasone, insulin, and indomethacin (*17*). Induction was apparent by the accumulation of lipid-rich vacuoles within cells (Fig. 2, A, D, and G). These adipocytes expressed peroxisome proliferation-activated receptor γ2 (PPARγ2), lipoprotein lipase (LPL), and the fatty acid–binding protein aP2 (*18*) (see Web Fig. 2, available at www.sciencemag.org/feature/data/983855.shl). Multiple induction treatments resulted in more than 95% of the cells committing to this lineage, and the lipid vacuoles continued to develop over time, coalesced, and eventually filled the cell. These adipocytes remained healthy in culture for at least 3 months.

To promote chondrogenic differentiation, we gently centrifuged the isolated mesenchymal cells to form a pelleted micromass and cultured the cells without serum and with transforming growth factor–β3 (*19*). The cell pellets developed a multilayered matrix-rich morphology and histologically showed an increased proteoglycan-rich extracellular matrix during culture. Type II collagen (Fig. 2, B, E, and H), which is typical of articular cartilage, was detected at 10 to 14 days with monoclonal C4F6 (*20*). For each donor, the cells showed a positive stain for chondrocytic markers over an increasing proportion of the pellet from 10 to 21 days, and this persisted without decreasing. Similar cultures have been maintained for 3 months. Chondrocyte-like lacunae were evident in histological sections, and the extensive extracellular matrix was rich in aggrecan and type II collagen (see

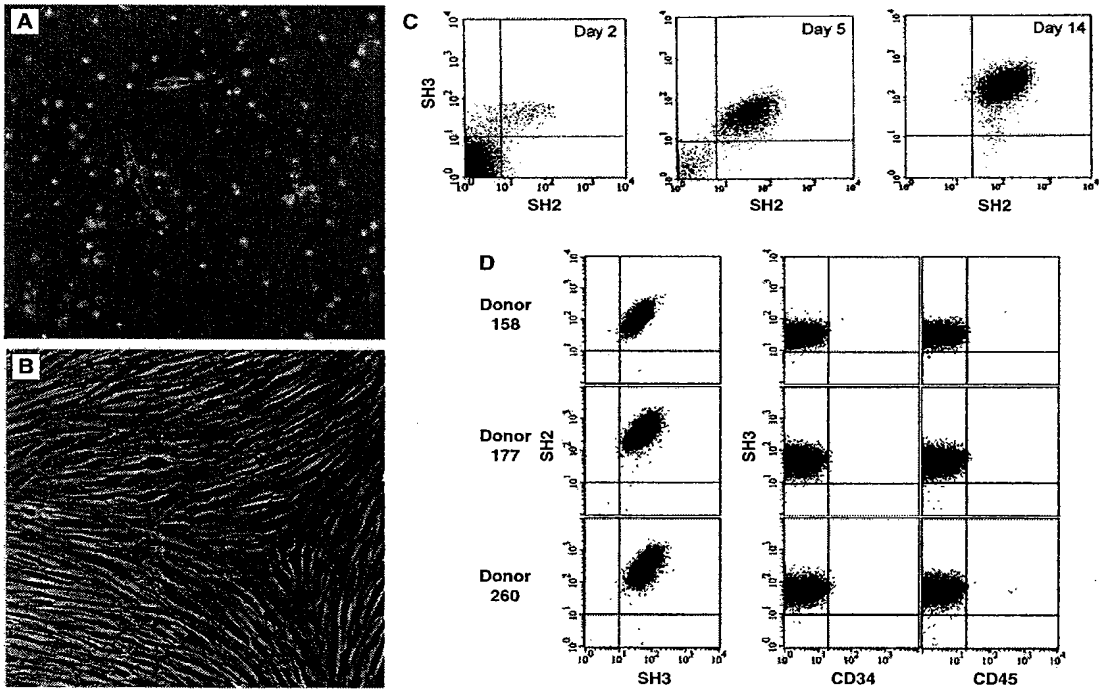

Fig. 1. Characterization of isolated marrow stromal cells. Cells were cultured from marrow after density fractionation and are shown (**A**) at 48 hours after plating and (**B**) at 10 days after plating. (**C**) Flow cytometry shows the enrichment of these cells as they were cultured. Results shown were obtained at days 2, 5, and 14 of culture with antibodies SH2 and SH3, which were raised against surface markers (*11*). At 14 days, the cells were 95 to 99% homogeneous and were negative for reactivity to antigens CD14, CD34 (Becton-Dickinson), or CD45 (Pharmingen), which are common on cells of the hematopoietic lineages. (**D**) Homogeneity and reproducibility of the isolation procedure was demonstrated by flow cytometry. See Web Fig. 1 for additional information.

Web Fig. 3, available at www.sciencemag.org/feature/data/983855.shl).

The osteogenic differentiation of cultured human mesenchymal cells that were derived from adult bone marrow has been characterized (*3, 21*). Under the influence of dexamethasone, β-glycerol phosphate, and ascorbate and in the presence of 10% v/v FBS, the isolated mesenchymal cells formed aggregates or nodules and increased their expression of alkaline phosphatase (Fig. 2, C, F, and I). Quantitative assays revealed a 4- to 10-fold increase in alkaline phosphatase activity, and calcium accumulation was evident after 1 week and increased over time (see Web Fig. 4, available at www.sciencemag.org/feature/data/983855.shl).

As differentiation to the three lineages occurred, there was no evidence of necrosis or apoptosis; it is apparent when groups of dead cells are present because there are no scavenger cells to remove them. However, we cannot rule out the fact that apoptosis may occur on a single-cell basis.

In contrast, cultured normal skin fibroblasts did not undergo any such differentiation when cultured for as long as 28 days, although the cells appeared healthy and nonnecrotic in these different conditions (Fig. 2, K and N). Cultured hMSCs, therefore, had a differentiation capacity that was not present in primary fibroblasts, which are mature mesenchymal cells.

The entire culture of expanded mesenchymal cells appeared to progress to the desired lineage, on the basis of phenotypic characterization and histological analysis. Multiple lineages were not present. To further test the possibility that a barely detectable population of cells could differentiate to lineages other than those desired in the in vitro assays, we isolated RNA from cells after differentiation, and reverse transcriptase–polymerase chain reaction (RT-PCR) was used to amplify expressed transcripts from multiple genes whose expression is restricted to the adipocytic (PPARγ2 and aP2), chondrocytic (type II and IX collagens), or osteocytic (osteopontin and alkaline phosphatase) lineage (see Web Fig. 5, available at www.sciencemag.org/feature/data/983855.shl). The sensitive RT-PCR assays, in addition to the immunological and histochemical data, showed that neither the adipogenic nor the osteogenic cultures were composed of cells of multiple lineages. The chondrogenic cultures did not appear histologically to contain cells that were of the other lineages, but they did express osteopontin and alkaline phosphatase.

These experiments showed that the isolated expanded hMSC culture would differentiate, in a controlled manner, to multiple lineages. To test the hypothesis that marrow contains individual hMSCs that could differentiate to all three of the lineages and to rule out that marrow contains only committed progenitor cells, we performed the same experiments with expanded colonies of cells derived from single cells. For this, the Percoll-isolated marrow cells were plated at 1.5 million to 6 million cells per 150-mm dish. Individual adherent cells were identified at 24 hours and grown into colonies of 30 to 100 cells, and the colonies were isolated with cloning rings. Isolated colonies were treated with trypsin and transferred to individual wells of a 24-well tissue culture plate and then transferred to a 75-cm^2 flask as they expanded. Approximately 800,000 to 1,500,000 cells were obtained from the flasks at harvest, representing 19 to 21 in vitro population doublings from the original cell. The cells were subjected to flow cytometric analysis and in vitro differentiation assays.

Flow analysis of the colonies revealed the same surface molecules as those found on the cultured undifferentiated hMSCs from which they were derived (Fig. 3) and on the other donors that were studied (Fig. 1). Of the six colonies derived from clonal cells, all underwent osteogenic differentiation, five underwent adipogenic differentiation, and two also underwent chondrogenic differentiation (Fig. 4). One other colony was weakly but clearly positive for the chondrocytic phenotype. The fact that some of the marrow-derived adult human mesenchymal cells, which were grown and expanded as individual colonies, possessed a multipotent capacity for lineage differentiation supports our conclusion that these cells represent human mesenchymal stem cells (hMSCs). The observation that some colonies displayed limited differentiation under these experimental conditions has several possible interpretations. For example, the clonal cell isolation, 19 to 21 population doublings, and in vitro culture conditions may have caused some loss of multilineage potential that was originally present in these cells. Another interpretation is that some of these cells might represent progenitor cells, with restricted differentiation potential, that are present in adult marrow.

The specific environmental cues to initiate the proliferation and differentiation of hMSCs in vivo are not understood. The ability to isolate, expand the culture, and direct the differentiation of hMSCs in vitro to particular lineages provides the opportunity to study events associated with commitment and dif-

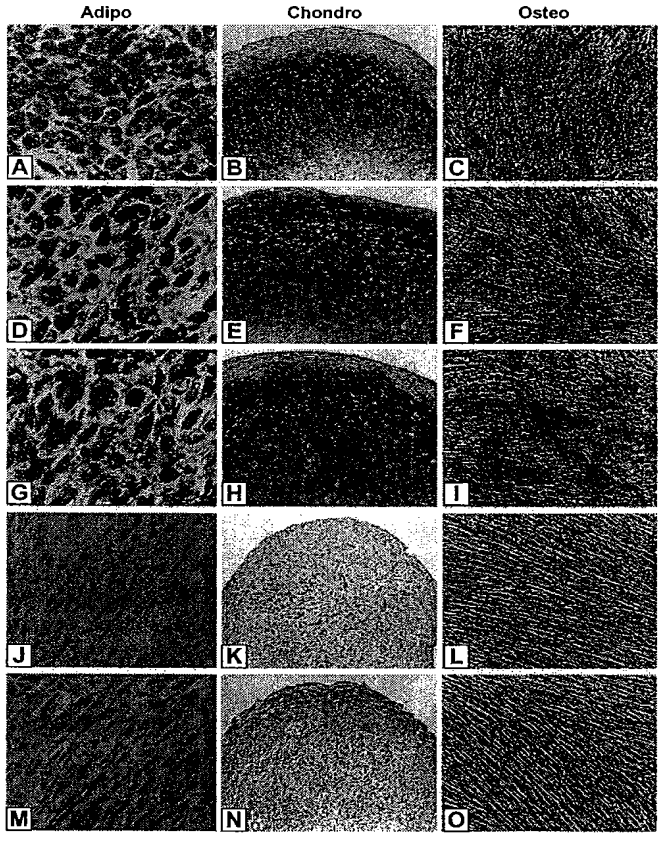

Fig. 2. Isolated marrow-derived stem cells differentiate to mesenchymal lineages. Cultured cells from donors were tested for the ability to differentiate in vitro to multiple lineages. Donors (**A** through **C**) 158, (**D** through **F**) 177, and (**G** through **I**) 260 were each shown to differentiate appropriately to the adipogenic (Adipo), chondrogenic (Chondro), and osteogenic (Osteo) lineages. Adipogenesis was indicated by the accumulation of neutral lipid vacuoles that stain with oil red O (A, D, and G), and such changes were not evident (**J**) with Hs27 newborn skin fibroblasts or (**M**) with 1087Sk adult mammary tissue fibroblasts. Chondrogenesis was shown by staining with the C4F6 monoclonal antibody to type II collagen and by morphological changes (B, E, and H), which were not seen by similarly culturing (**K**) Hs27 or (**N**) 1087Sk cells. Osteogenesis was indicated by the increase in alkaline phosphatase (C, F, and I) and calcium deposition, which was not seen in the (**L**) Hs27 or (**O**) 1087Sk cells (see Web Fig. 4).

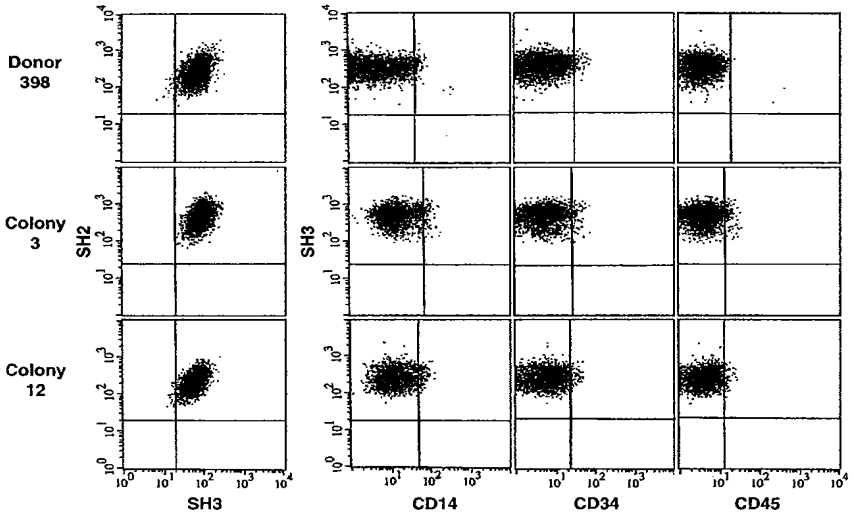

Fig. 3. Flow cytometry characterization of clonal cells. Marrow stromal cells from donor 398 were plated at low density, and individual attached cells were identified on the culture dish. When a colony was evident, a cloning ring was placed around it, and the colony was subcultured to an individual well of a 24-well culture plate. The expanded cells were transferred to a 75-cm^2 flask, analyzed when they approached confluence, and compared to the parent cells. Colony cells were stained with surface markers SH3 and SH2 or CD14, CD34, or CD45 and found to be homogeneous and indistinguishable from the parent culture. Cells of colonies 3 and 12 were multipotential in the differentiation assays (as shown in Fig. 4).

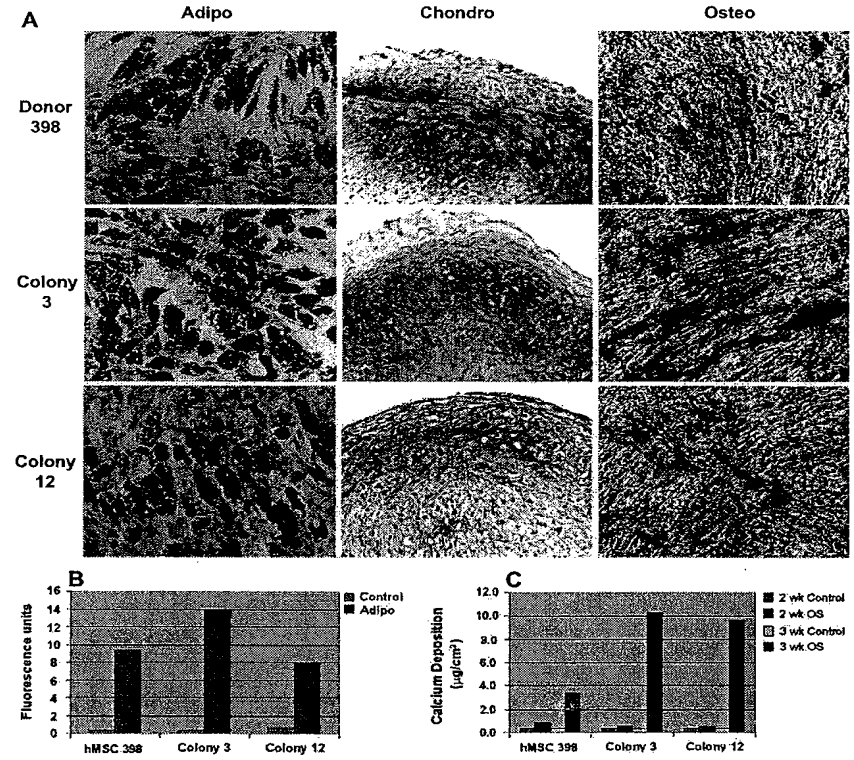

Fig. 4. Comparison of the differentiation potential of parental and clonally derived cells. **(A)** Cells of colonies 3 and 12 were placed in the differentiation conditions and were shown to give rise to adipogenic, chondrogenic, and osteogenic lineages. The response was very similar to the parental cell population. The colonies also gave a similar response in the quantitative assays for **(B)** adipogenic lipid accumulation and **(C)** osteogenic calcium deposition (OS).

ferentiation. From the different assay conditions required for efficient differentiation, we conclude that basal nutrients, cell density, spatial organization, mechanical forces, and growth factors and cytokines have a profound influence on hMSC differentiation. The hMSCs cultured in each of the differentiation conditions may also produce autocrine and paracrine factors that are essential for lineage progression. As for the differentiation to other mesenchymal lineages, expanded mesenchymal cells have been shown to function as stromal cells for the in vitro support of HSCs (*13*), and rabbit MSCs have been shown to be effective for the regeneration of a severed tendon in a rabbit model (*8*).

The hMSCs described here have the ability to proliferate extensively, and they maintain the ability to differentiate into multiple cell types in vitro, establishing their stem cell nature. Their cultivation and selective differentiation should provide further understanding of this important progenitor of multiple tissue types and the potential of new therapeutic approaches for the restoration of damaged or diseased tissue.

References and Notes

1. J. A. Thomson *et al.*, *Science* **282**, 1145 (1998); M. J. Shamlott *et al.*, *Proc. Natl. Acad. Sci. U.S.A.* **95**, 13726 (1998).
2. J. E. Till and E. A. McCulloch, *Radiat. Res.* **14**, 213 (1961); B. I. Lord, in *Stem Cells*, C. S. Potten, Ed. (Academic Press, New York, 1996), pp. 401–422; C. I. Civin *et al.*, *J. Immunol.* **133**, 157 (1984).
3. S. A. Kuznetsov *et al.*, *J. Bone Miner. Res.* **12**, 1335 (1997); D. J. Prockop, *Science* **276**, 71 (1997); R. F. Pereira *et al.*, *Proc. Natl. Acad. Sci. U.S.A.* **92**, 4857 (1995); A. I. Caplan, *J. Orthop. Res.* **9**, 641 (1991); A. J. Friedenstein, *Int. Rev. Cytol.* **47**, 327 (1976); M. Owen and A. J. Friedenstein, in *Cell and Molecular Biology of Vertebrate Hard Tissues*, D. Evered and S. Harnett, Eds. (Wiley, Chichester, UK, 1988), pp. 42–60.
4. A. J. Friedenstein, R. K. Chailakhyan, U. V. Gerasimov, *Cell Tissue Kinet.* **20**, 263 (1987); B. Ashton *et al.*, *Clin. Orthop. Relat. Res.* **151**, 294 (1980); I. Bab, C. R. Howlett, B. A. Ashton, M. E. Owen, *ibid.* **187**, 243 (1984).
5. S. E. Haynesworth, J. Goshima, V. M. Goldberg, A. I. Caplan, *Bone* **13**, 81 (1992).
6. R. J. Bergman *et al.*, *J. Bone Miner. Res.* **11**, 568 (1996); J. E. Dennis and A. I. Caplan, *Connect. Tissue Res.* **35**, 93 (1996); Q. Cui, G.-J. Wang, G. Balian, *J. Bone Joint Surg. Am. Vol.* **79A**, 1054 (1997); S. Wakitani, T. Saito, A. I. Caplan, *Muscle Nerve* **18**, 1417 (1995).
7. P. Cassiede, J. E. Dennis, F. Ma, A. I. Caplan, *J. Bone Miner. Res.* **11**, 1264 (1996); A. E. Grigoriadis, J. N. M. Heersche, J. E. Aubin, *J. Cell Biol.* **106**, 2139 (1988); P. S. Leboy, J. N. Beresford, C. Devlin, M. E. Owen, *J. Cell. Physiol.* **146**, 370 (1991); J. J. Bellows and J. E. Aubin, *Dev. Biol.* **133**, 8 (1989).
8. R. G. Young *et al.*, *J. Orthop. Res.* **16**, 406 (1998).
9. S. Wakitani *et al.*, *J. Bone Joint Surg. Am. Vol.* **76A**, 579 (1994); B. Johnstone, T. M. Hering, A. I. Caplan, V. M. Goldberg, J. U. Yoo, *Exp. Cell Res.* **238**, 265 (1998).
10. S. Kadiyala, R. D. Young, M. A. Thiede, S. P. Bruder, *Cell Transplant.* **6**, 125 (1997); S. P. Bruder, K. H. Kraus, V. M. Goldberg, S. Kadiyala, *J. Bone Joint Surg. Am. Vol.* **80A**, 985 (1998).
11. D. P. Lennon *et al.*, *In Vitro Cell. Dev. Biol.* **32**, 602 (1996); S.-L. Cheng *et al.*, *Endocrinology* **134**, 277 (1994).

12. S. E. Haynesworth, M. A. Baber, A. I. Caplan, *Bone* **13**, 69 (1992).
13. M. K. Majumdar *et al.*, *J. Cell. Physiol.* **176**, 57 (1998).
14. S. P. Bruder *et al.*, *Clin. Orthop. Relat. Res.* **355S**, S247 (1998).
15. R. Bucala, L. A. Spiegel, J. Chesney, M. Hogan, A. Cerami, *Mol. Med.* **1**, 71 (1994).
16. These fibroblasts represented middle passage newborn foreskin fibroblasts (Hs27), which were obtained at passage 14 from the American Type Culture Collection (ATCC), and early passage adult skin fibroblasts (1087Sk), which were obtained at passage 1 from ATCC, both with normal karyotype.
17. M. F. Pittenger, U.S. Patent 5, 827, 740 (1998).
18. Murine cDNA probes for LPL and PPARγ2 were the gift of J. Gimble (University of Oklahoma, School of Medicine, Oklahoma City). Polyclonal antibody to aP2 was provided by M. D. Lane (Johns Hopkins University, School of Medicine, Baltimore, MD).
19. A. M. Mackay, S. C. Beck, J. M. Murphy, F. P. Barry, M. F. Pittenger, *Tissue Eng.* **4**, 472 (1998); J. U. Yoo *et al.*, *J. Bone Joint Surg. Am. Vol.* **80A**, 1745 (1998).
20. G. R. Srinivas, H. J. Barrach, C. O. Chichester, *J. Immunol. Methods* **159**, 53 (1994).
21. S. P. Bruder, N. Jaiswal, S. E. Haynesworth, *J. Cell. Biochem.* **64**, 278 (1997); N. Jaiswal, S. E. Haynesworth, A. I. Caplan, S. P. Bruder, *ibid.*, p. 295; S. P. Bruder *et al.*, *J. Bone Miner. Res.* **13**, 655 (1998).
22. We thank D. Fink, J. Andres, R. Deans, F. Barry, S, Bruder, M. Thiede, A. Moseley, and J. Burns for discussion and review of the manuscript; M. Black and M. Earlington for cell isolation from marrow; and D. Sterchi, D. Brown, and J. Skwarek for histology. This work was supported by Osiris Therapeutics (www.osiristx.com) and, in part, by a research contract from the Defense Advanced Research Projects Agency.

22 January 1999; accepted 4 March 1999

Two Distinct Cytokines Released from a Human Aminoacyl-tRNA Synthetase

Keisuke Wakasugi and Paul Schimmel*

Aminoacyl-tRNA synthetases catalyze aminoacylation of transfer RNAs (tRNAs). It is shown that human tyrosyl-tRNA synthetase can be split into two fragments with distinct cytokine activities. The endothelial monocyte–activating polypeptide II–like carboxy-terminal domain has potent leukocyte and monocyte chemotaxis activity and stimulates production of myeloperoxidase, tumor necrosis factor-α, and tissue factor. The catalytic amino-terminal domain binds to the interleukin-8 type A receptor and functions as an interleukin-8–like cytokine. Under apoptotic conditions in cell culture, the full-length enzyme is secreted, and the two cytokine activities can be generated by leukocyte elastase, an extracellular protease. Secretion of this tRNA synthetase may contribute to apoptosis both by arresting translation and producing needed cytokines.

Aminoacyl-tRNA synthetases are ancient proteins that are essential for decoding genetic information in translation. In higher eukaryotes, nine aminoacyl-tRNA synthetases associate with at least three other polypeptides to form a supramolecular multienzyme complex (*1*). Each of these nine eukaryotic tRNA synthetases has an additional domain appended to the NH_2- or COOH-terminal end of the core enzyme, which itself is closely related to the respective prokaryotic counterpart (*2*). In most cases, the appended domains appear to contribute to the assembly of the multienzyme complex (*2*). However, the presence of an extra domain is not strictly correlated with the association of a synthetase into the multienzyme complex. For example, human tyrosyl-tRNA synthetase (TyrRS) has an extra domain at the COOH-terminus compared to prokaryotic and lower eukaryotic TyrRSs (Fig. 1) (*3*), and bovine and rabbit TyrRSs are also suggested to contain an extra domain (*4*). Yet, higher eukaryotic TyrRS is not a component of the multienzyme complex (*1*). Interestingly, the COOH-terminal domain of human TyrRS has 51% sequence identity to the mature form of human endothelial monocyte–activating polypeptide II (EMAP II) (*3*). TyrRS is the only higher eukaryotic aminoacyl-tRNA synthetase known to contain an EMAP II–like domain. In initial experiments, we found that this domain was dispensable for aminoacylation in vitro and in yeast (*5–7*).

EMAP II is a proinflammatory cytokine that was initially identified as a product of murine methylcholanthrene A–induced fibrosarcoma cells (*8*). Pro–EMAP II is cleaved and is secreted from apoptotic cells to produce a biologically active 22-kD mature cytokine (*8, 9*). The mature EMAP II can induce migration of mononuclear phagocytes (MPs) and polymorphonuclear leukocytes (PMNs); it also stimulates the production of tumor necrosis factor-α (TNFα) and tissue factor by MPs and the release of myeloperoxidase from PMNs (*8*).

We investigated each of these five activities with the cloned COOH-terminal domain of human TyrRS and with the full-length enzyme that contains the COOH-terminal domain fused to the catalytic core (*5*). The COOH-terminal domain induced migration of human MPs from peripheral blood (*10*) to an extent comparable to that seen with mature human EMAP II (Fig. 2A). In contrast, no chemotaxis was observed with the full-length TyrRS. The COOH-terminal domain of TyrRS also stimulated TNFα and MP tissue factor activities (Fig. 2, A and B), induced release of PMN myeloperoxidase activity in the peroxidase generation assay (Fig. 2B), and induced PMN migration in chemotaxis chambers (Fig. 2C). The induction of PMN migration by the COOH-terminal domain and mature EMAP II showed the bell-shaped concentration dependence that is characteristic of chemotactic cytokines (*7, 11*). Human full-length TyrRS had none of these properties (Fig. 2, B and C).

We also investigated the NH_2-terminal catalytic domain (mini TyrRS) in the same assays. Human "mini" TyrRS did not induce migration of MPs and did not stimulate TNFα and tissue factor production by MPs (Fig. 2, A and B). Surprisingly, incubation of PMNs with mini TyrRS induced PMN migration (Fig. 2C), and this activity showed a bell-shaped concentration dependence (*7*).

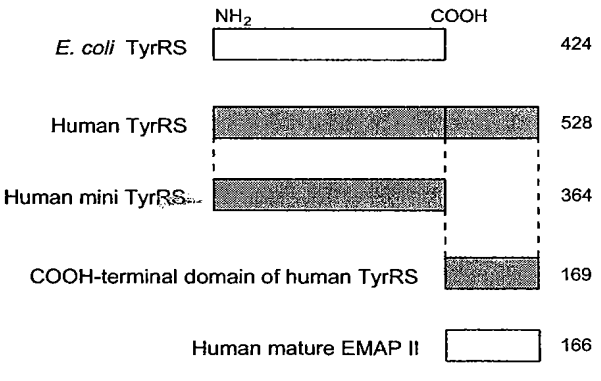

Fig. 1. Schematic representation of the TyrRS constructs used in this study. Alignments of truncated human TyrRSs with human full-length TyrRS (*3, 25*), *E. coli* TyrRS (*26*), and mature human EMAP II (*8*) are depicted schematically. Numbers at right indicate protein size in amino acids.

The Skaggs Institute for Chemical Biology, The Scripps Research Institute, Beckman Center, 10550 North Torrey Pines Road, La Jolla, CA 92037, USA.

*To whom correspondence should be addressed. E-mail: schimmel@scripps.edu